# Bath-Optimized Minimal-Energy Protection of Quantum Operations from Decoherence

Jens Clausen, Guy Bensky, and Gershon Kurizki
*Department of Chemical Physics, Weizmann Institute of Science, Rehovot, 76100, Israel*
(Received 23 September 2009; published 25 January 2010)

We put forward a general strategy for dynamic control that ensures bath-optimized fidelity of a desired multidimensional quantum operation in the presence of non-Markovian baths and noises with stationary autocorrelations. It benefits from the vast freedom of arbitrary, not just pulsed, time-dependent control. This allows the dramatic reduction of the invested energy and the corresponding error compared to pulsed control.

DOI: 10.1103/PhysRevLett.104.040401 PACS numbers: 03.65.Yz, 02.70.−c, 03.67.Pp

*Introduction.*—The quest for strategies for combating decoherence is of paramount importance to the control of open quantum systems, particularly for quantum information operations [1]. A prevailing unitary strategy aimed at suppressing decoherence is dynamical decoupling (DD) [2–4], which consists, in the case of a qubit, in the application of strong and fast pulses alternating along orthogonal Bloch-sphere axes, e.g., $X$ and $Z$. In the frequency domain, where the decoherence rate can be described as overlap between the spectra of the pulse-driven (modulated) system and the bath [5], DD is tantamount to shifting the driven-system resonances beyond the bath cutoff frequencies. DD control is inherently pulsed, although it can invoke bandwidth considerations for pulses to maximize the speed and fidelity of quantum gate operations [2,3].

Here we put forward an altogether different universal strategy: bath-optimal minimal-energy control (BOMEC) of multidimensional quantum operations subject to any given noise or bath with stationary autocorrelations. It draws upon the vast additional freedom of arbitrary (not just pulsed) Hamiltonian time dependence. This allows the reduction (by orders of magnitude) of the invested energy compared to pulsed control. This approach ensures bath-optimized effective decoherence control under constraints imposed by the non-Markov bath response. It tackles the fidelity deterioration with control energy, a key effect that has been hitherto unexplored. The price we pay is the need for at least partial knowledge of the bath or noise spectrum, which is experimentally accessible [6] without the need for microscopic models. In this sense, BOMEC is a major generalization of dynamic control by modulation developed for qubit dephasing [7].

*Gate error.*—We assume that the system Hamiltonian $\hat{H}_S(t)$ implements a desired quantum gate operation at time $t$, and aim at designing it so as to minimize the decoherence and noise errors [2,3]. The system-bath interaction $\hat{H}_I$ then acquires time dependence in the interaction picture under the action of $\hat{H}_S(t)$ and the bath Hamiltonian $\hat{H}_B$. Assuming factorized initial states of the system and the bath, $\hat{\varrho}_{\mathrm{tot}}(0) = \hat{\varrho}(0) \otimes \hat{\varrho}_B$, tracing over the bath, and further assuming that $\mathrm{Tr}_B(\hat{H}_I\hat{\varrho}_B) = \hat{0}$, $\mathrm{Tr}_S\hat{H}_I = \hat{0}$ yields for the system state $\hat{\varrho}(t)$ the following deviation from the initial state in the interaction picture [8]

$$\begin{aligned}\hat{\varrho}(t) &= \hat{\varrho}(0) - \Delta\hat{\varrho}(t),\\ \Delta\hat{\varrho}(t) &= \int_0^t dt_1 \int_0^{t_1} dt_2 \mathrm{Tr}_B[\hat{H}_I(t_1), [\hat{H}_I(t_2), \hat{\varrho}_{\mathrm{tot}}(t_2)]].\end{aligned} \tag{1}$$

In what follows, we assume that up to $t$, the combined system-bath state changes only weakly compared to $\hat{H}_I$, so that we approximate in (1) $\hat{\varrho}_{\mathrm{tot}}(t_2) \approx \hat{\varrho}_{\mathrm{tot}}(0)$ in the integral. This means that the control is assumed effective enough to allow only small errors, consistently with the second order approximation of both the Nakajima-Zwanzig and the time-convolutionless non-Markov master equations [9,10].

To justify this assumption, we try to reduce the discrepancy between the states evolved for time $t$ in the presence and absence of the bath by minimizing $\langle\Delta\hat{\varrho}(t)\rangle \equiv \langle\Psi|\Delta\hat{\varrho}_\Psi(t)|\Psi\rangle$ averaged over all initial states $\hat{\varrho}_\Psi(0) = |\Psi\rangle\langle\Psi|$. For a $d$-level system this averaging yields our measure of decoherence (error) in the form [8,11]

$$\begin{aligned}\overline{\langle\Delta\hat{\varrho}(t)\rangle} &= 2\kappa\mathrm{Re}\int_0^t dt_1 \int_0^{t_1} dt_2 \langle\hat{H}_I(t_1)\hat{H}_I(t_2)\rangle_{\mathrm{SB}}\\ &= \kappa\Big\langle\Big[\int_0^t dt_1 \hat{H}_I(t_1)\Big]^2\Big\rangle_{\mathrm{SB}},\end{aligned} \tag{2}$$

where $\kappa = 1 - (d+1)^{-1}$, $\langle\cdot\rangle_{\mathrm{SB}} = d^{-1}\mathrm{Tr}_{\mathrm{SB}}[(\cdot)\hat{\varrho}_B]$. Equation (2) provides a fundamental insight: the ensemble-averaged error $\overline{\langle\Delta\hat{\varrho}(t)\rangle}$ is proportional to the mean square of the system-bath interaction energy in the (instantaneous) interaction picture. For worst-case error minimization cf. [8].

Since our aim is to suppress $\overline{\langle\Delta\hat{\varrho}(t)\rangle}$ by system manipulations alone, we now separate system and bath parts by decomposing any interaction Hamiltonian in an appropriate orthogonal basis as

$$\hat{H}_I = \sum_{j=1}^{d^2-1} \hat{B}_j \otimes \hat{S}_j, \tag{3}$$

where $\hat{S}_j$ are the system (traceless) basis operators obeying $\mathrm{Tr}(\hat{S}_j\hat{S}_k) = 2\delta_{jk}$ and $\hat{B}_j$ are bath operators that satisfy

 

$\langle \hat{B}_j \rangle_B = \mathrm{Tr}_B(\hat{B}_j \hat{\varrho}_B) = 0$ and carry no explicit time dependence. For every $\hat{S}_j$ basis there exists a unique decomposition of the system-bath Hamiltonian in this form. In the interaction picture

$$\hat{B}_j(t) = e^{i\hat{H}_B t}\hat{B}_j e^{-i\hat{H}_B t}, \qquad \hat{S}_j(t) = \hat{U}^\dagger(t)\hat{S}_j\hat{U}(t), \quad (4)$$

where $\hat{U}(t) = T_+ e^{-i\int_0^t dt' \hat{H}_S(t')}$. We shall minimize $\overline{\langle \Delta\hat{\varrho}(t)\rangle}$ for a given, experimentally accessible [6], bath correlation matrix $\underline{\mathbf{\Phi}}(t)$ defined as

$$\Phi_{jk}(t) = \langle \hat{B}_j(t)\hat{B}_k\rangle_B, \quad (5)$$

by searching for an appropriate system-modulation matrix $\underline{\boldsymbol{\epsilon}}(t)$ defined as

$$\epsilon_{jk}(t) = \tfrac{1}{2}\mathrm{Tr}[\hat{S}_j(t)\hat{S}_k], \quad (6)$$

which describes the rotation of the system basis due to the modulation: $\hat{S}_j(t) = \sum_{k=1}^{d^2-1}\epsilon_{jk}(t)\hat{S}_k$.

It is expedient to define the decoherence matrix

$$\underline{\boldsymbol{R}}(t_1, t_2) = \underline{\boldsymbol{\epsilon}}^T(t_1)\underline{\mathbf{\Phi}}(t_1 - t_2)\underline{\boldsymbol{\epsilon}}(t_2) \quad (7)$$

as a matrix product obeying $\underline{\boldsymbol{R}}^\dagger(t_1, t_2) = \underline{\boldsymbol{R}}(t_2, t_1)$. This decoherence matrix, transformed to the instantaneous rotating frame, is at the heart of the treatment.

By algebraic manipulations, we can rewrite (2) as

$$\overline{\langle \Delta\hat{\varrho}(t)\rangle} = 2\frac{\kappa}{d}\int_0^t dt_1 \int_0^t dt_2 \mathrm{Tr}\underline{\boldsymbol{R}}(t_1, t_2). \quad (8)$$

Alternatively, we can express (8) as

$$\overline{\langle \Delta\hat{\varrho}(t)\rangle} = 4t\frac{\kappa}{d}\int_0^\infty d\omega \mathrm{Tr}[\underline{\boldsymbol{G}}(\omega)\underline{\boldsymbol{F}}_t(\omega)], \quad (9)$$

where $\underline{\boldsymbol{G}}(\omega) = \int_{-\infty}^\infty dt e^{i\omega t}\mathrm{Re}\underline{\mathbf{\Phi}}(t)$, $\underline{\boldsymbol{F}}_t(\omega) = t^{-1}\underline{\boldsymbol{\epsilon}}_t(\omega)\underline{\boldsymbol{\epsilon}}_t{}^\dagger(\omega)$, and $\underline{\boldsymbol{\epsilon}}_t(\omega) = (1/\sqrt{2\pi})\int_0^t d\tau e^{i\omega\tau}\underline{\boldsymbol{\epsilon}}(\tau)$. Hence, the error is the spectral overlap of two matrix-valued functions: the bath-coupling spectral matrix $\underline{\boldsymbol{G}}(\omega)$, and the finite time system-modulation spectral matrix $\underline{\boldsymbol{F}}_t(\omega)$ [cf. (7)]. In (9) we have made use of the fact that $\underline{\mathbf{\Phi}}(-t) = \underline{\mathbf{\Phi}}^\dagger(t)$, so that it is sufficient to integrate over positive frequencies.

Equation (9) constitutes a generalization of the "universal formula" [5] to arbitrary multidimensional systems and baths. It provides a major insight: the system and bath spectra (all matrix components) must be anticorrelated; i.e., $G_{jk}(\omega)$ minima must coincide with $(F_t)_{jk}(\omega)$ maxima and vice versa to minimize the mean error (9), as illustrated below. Certain components $G_{jk}(\omega)$, $(F_t)_{jk}(\omega)$ may be negative or complex. This may allow us to "destructively interfere" their contributions, i.e., engineer "decoherence-free" subspaces [12]. These prospects of our general approach can be used for entanglement protection [13].

*Decoherence minimization.*—Our goal is to find a system Hamiltonian $\hat{H}_S(t)$, $0 \le t \le T$, implementing a given unitary gate $\hat{U}(T)$ at a fixed time $T$. This requires minimizing the bath-induced state error (2) or (8) in the interaction picture under $\hat{H}_S(t)$. We may similarly account for the effects of modulation or control noise, in addition to bath noise [8].

The major difficulty in minimizing (8) using (4)–(6) is that (4) involves time-ordered integration for noncommuting control operators along different axes. To circumvent this difficulty, we use $\hat{U}(t)$ as our basic object instead of $\hat{H}_S(t)$, and assume a parametrization $\hat{U}[f_l(t), t]$ in terms of a set of real parameters $f_l(t)$, which we combine to a vector $\underline{\boldsymbol{f}}(t)$. The boundary values $\underline{\boldsymbol{f}}(0)$ and $\underline{\boldsymbol{f}}(T)$ should be such that $\hat{U}(t = 0) = \hat{I}$ and $\hat{U}(t = T)$ is the desired gate.

If the bath-coupling spectrum $\underline{\boldsymbol{G}}(\omega)$ vanishes (has cutoff) at any high frequency, the overlap (9) can be presumed arbitrarily small under sufficiently rapid modulation of the Hamiltonian, such that all components of $\underline{\boldsymbol{F}}_t(\omega)$ are shifted beyond this cutoff, thus achieving DD [2–4]. Yet this may require a diverging system energy. A consideration seldom taken into account is that fidelity generally drops with modulation energy, as discussed below. We therefore impose an energy constraint on the modulated system

$$E_S = \int_0^T dt_1 \langle \hat{H}_S^2(t_1)\rangle_S = \mathrm{const}, \quad (10)$$

where $\langle\cdot\rangle_S = d^{-1}\mathrm{Tr}_S(\cdot)$ [cf. (2)]. An alternative constraint

$$E = \int_0^T dt_1 |\dot{\underline{\boldsymbol{f}}}(t_1)|^2 = \mathrm{const} \quad (11)$$

is on the bandwidth: $E$ accounts for the fact that the time dependence of a parametrization cannot be arbitrarily fast and hence bounds the modulation energy $E_S$.

The minimization of (8) subject to (11) is an extremal problem in terms of the controls $\underline{\boldsymbol{f}}$. The stationary condition can be formulated in terms of a Lagrange multiplier $\lambda$ as $\underline{\boldsymbol{\delta}}\overline{\langle \Delta\hat{\varrho}(t)\rangle} + \lambda\underline{\boldsymbol{\delta}}E = 0$, where $\underline{\boldsymbol{\delta}}$ is the total variation with respect to $\underline{\boldsymbol{f}}$. Then, using the parametrization $\underline{\boldsymbol{\nabla}}_{t_1} \equiv \{\frac{\partial}{\partial f_l(t_1)}\}$ in $\underline{\boldsymbol{R}}$ [Eq. (7)], yields the Euler-Lagrange equation

$$\ddot{\underline{\boldsymbol{f}}}(t_1) = \lambda\underline{\boldsymbol{g}}(t_1), \qquad \underline{\boldsymbol{g}}(t_1) \equiv \int_0^T dt_2 \underline{\boldsymbol{\nabla}}_{t_1}\mathrm{Re}\,\mathrm{Tr}\underline{\boldsymbol{R}}(t_1, t_2), \quad (12)$$

where $\lambda$ is related to the constraint (11) on $E$ [8].

We conclude the general treatment by recapitulating on the steps to find the optimal modulation of $\hat{H}_S(t_1)$: (i) After choosing the gate time $T$ and gate operation $\hat{U}(T)$, we declare a set of parameters $\underline{\boldsymbol{f}}$ controlling the evolution, such that $\hat{U}(t) = \hat{U}[\underline{\boldsymbol{f}}(t), t]$ which induces the instantaneous rotation matrix $\underline{\boldsymbol{\epsilon}}[\underline{\boldsymbol{f}}(t), t]$. We can now calculate $\underline{\boldsymbol{R}}(t_1, t_2)$ as a functional of $\underline{\boldsymbol{f}}$ via (4)–(6), using our knowledge of the bath (5). (ii) We now solve the Lagrange Eq. (12) for a given $\lambda$ using the boundary conditions, and calculate the error $\overline{\langle \Delta\hat{\varrho}(T)\rangle}$. (iii) The optimization is repeated for different values of $\lambda$ and $E_S$ in (10) is calculated for each solution. Among all solutions for which the error falls below a desired threshold value, we choose the one corresponding to the lowest $E_S$. (iv) The chosen solution $\underline{f}(t)$ is inserted into $\hat{U}[\underline{f}(t), t]$, yielding the instantaneous Hamiltonian

$$\hat{H}_S(t) = i\dot{\hat{U}}(t)\hat{U}^\dagger(t) = \sum_j \omega_j(t)\hat{S}_j. \quad (13)$$

*Application to a qubit.*—To apply the general procedure to a qubit for which $\hat{S}_j = \hat{\sigma}_j$ $(j = X, Y, Z)$ in (13), we resort to the Euler rotation-angle parametrization,

$$\hat{U}(t) = e^{-(i/2)f_3(t)\hat{\sigma}_3} e^{-(i/2)f_2(t)\hat{\sigma}_2} e^{-(i/2)f_1(t)\hat{\sigma}_3}.$$

In (13), $\omega_3(t)$ is now the level splitting, whereas $\omega_{1(2)}(t)$ are Rabi flipping rates. We choose two examples of uncorrelated baths (i.e., diagonal $\underline{\mathbf{\Phi}}$), namely, an Ohmic bath with different cutoffs in $X$, $Y$, $Z$, and a Lorentzian noise spectrum superposed with a second Lorentzian such that a spectral "hole" is obtained at different frequencies in $X$,

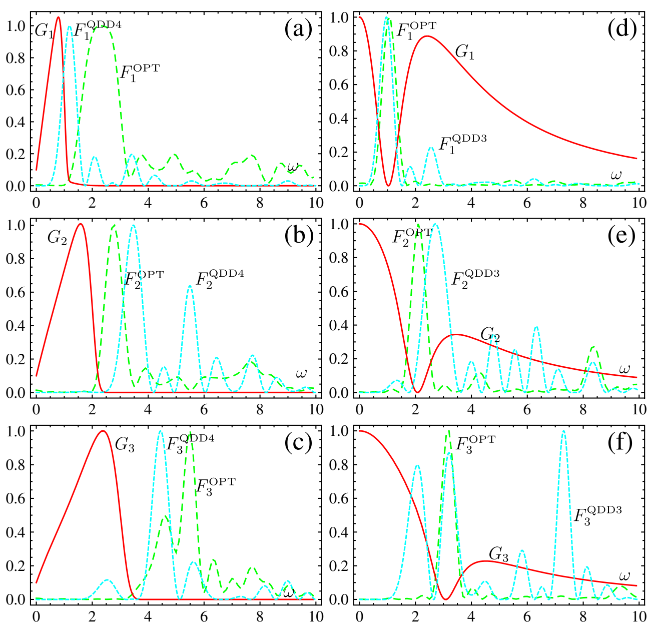


FIG. 1 (color online). Spectral overlaps between bath spectra $G_i(\omega)$ (solid red), modulation spectra $F_i^{\rm OPT}(\omega)$ (dashed green) for an optimized (BOMEC) storage (identity, 0) gate at $E_S = 130.5$ [(a),(b),(c)], and $E_S = 181.1$ [(d),(e),(f)], respectively, and modulation spectra $F_i^{\rm QDD}$ for pulse sequences [3] QDD4 [(a),(b),(c)] and QDD3 [(d),(e),(f)] (dotted blue), with $i = 1, 2, 3$ corresponding to $X$, $Y$, and $Z$ component, respectively. Graphs (a),(b),(c) represent an Ohmic bath spectrum with softened cutoff, whereas graphs (d),(e),(f) represent a Lorentzian spectrum with a dip. The optimal (BOMEC) modulation spectra $F_i^{\rm OPT}(\omega)$ are always anticorrelated with the bath spectra $G_i(\omega)$. By contrast, the DD pulse-sequence spectra are only anticorrelated with $G_i$ for Ohmic baths (a),(b),(c) but not for the bath spectra (d),(e),(f). The same is true for CUDD sequences [4].

$Y$, and $Z$. The corresponding bath-coupling spectra are shown in Fig. 1, along with our optimized modulation spectra, which are contrasted with DD pulse-sequence spectra.

The minimized gate error is shown in Fig. 2 as a function of the energy constraint (10) for both baths. Its comparison with the gate error obtained using various DD pulse sequences reveals two differences. The first concerns the energy scale: in rectangular DD pulse sequences, each $\pi$ pulse of duration $\tau$ contributes an amount $\pi^2/(4\tau)$ to (10), defining the basic energy scale of the DD method. This energy scale diverges for ideal pulses, $\tau \to 0$. By contrast, our approach assumes finite, much (2 orders of magnitude) smaller $E_S$. The second difference concerns energy monotonicity: DD sequences are designed *a priori*, regardless of the bath spectrum, and hence only significantly reduce the gate error if $E_S$ has risen above some threshold which is needed to shift all system frequencies beyond the bath cutoffs [4]. In contrast, our approach starts to reduce the gate error as soon as $E_S > 0$, since it optimizes the use of the available energy, by anticorrelating the modulation and bath spectra.

We next consider the gate fidelity limitations as a function of the control energy $E_S$ posed by leakage [14] to levels outside the relevant subspace (here a qubit). In a three-level $\Lambda$ system, any off-resonant control field acting

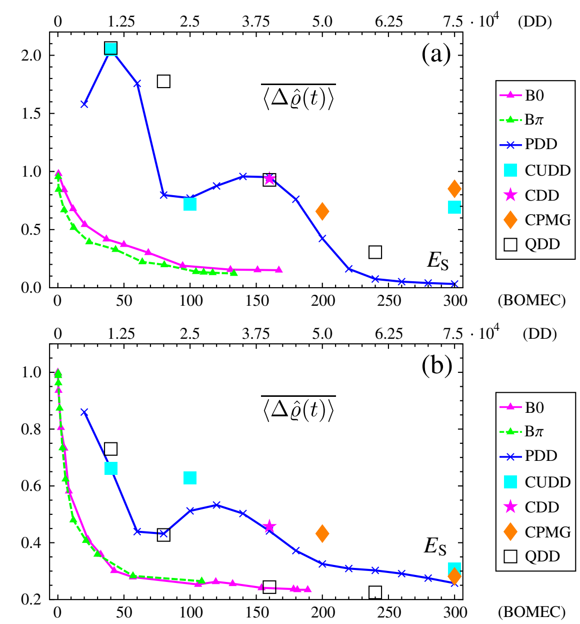


FIG. 2 (color online). Qubit gate error $\overline{\langle \Delta\hat{\varrho}(t)\rangle}$ scaled to unmodulated error, as a function of the energy constraint $E_S$ in units of the energy scale of each method (see text). Solid magenta (dashed green): optimized (BOMEC) storage (identity, $B0$) and flip ($B\pi$) gates, Solid blue: periodic $X$-$Z$ "bang bang" (2, 4, ..., 30 pulses). Separate points: DD pulse sequences [3,4]. (a) and (b) correspond to bath spectra shown on the left and right in Fig. 1. The energy scale of DD (top) is more than 2 orders of magnitude higher than that of BOMEC (bottom).

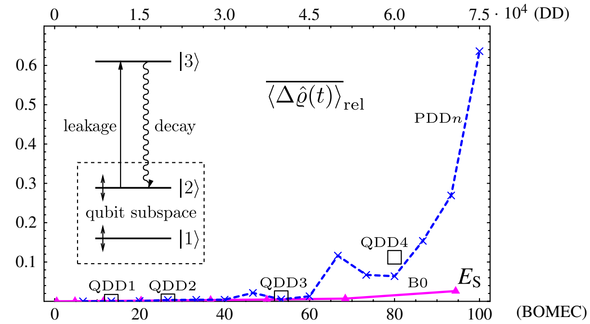


FIG. 3 (color online). Relative surplus error $\overline{\langle\Delta\hat{\varrho}(t)\rangle}_{\rm rel} = (\overline{\langle\Delta\hat{\varrho}(t)\rangle}_{\rm with} - \overline{\langle\Delta\hat{\varrho}(t)\rangle}_{\rm without})/\overline{\langle\Delta\hat{\varrho}(t)\rangle}_{\rm without}$ incurred by the inevitable leakage to the additional level $|3\rangle$ (inset) caused by the control as a function of the energy $E_S$, i.e., error with allowance for leakage compared to the error without (disregarding) leakage. Solid magenta: optimized (BOMEC) storage (identity, $B0$) gate. Dashed blue: periodic $X$-$Z$ "bang bang" $(2, 4, \ldots, 30$ pulses) and QDD as shown in Fig. 2(a) and a bath spectrum as shown in Fig. 1 (left). A (truncated) $1/\omega$ bath-coupling spectrum describes an amplitude coupling between levels $|2\rangle$ and $|3\rangle$ (leakage). The scales of $E_S$ are as in Fig. 2.

on the qubit levels $|1\rangle$, $|2\rangle$, causes leakage to the unwanted level $|3\rangle$ [15]. Such leakage and the ensuing incoherent decay $|3\rangle \rightarrow |2\rangle$ incur gate errors that grow with the control energy $E_S$. This behavior is illustrated in Fig. 3, which reveals that leakage error is more dramatic the more energetic the $\pi$-pulse sequences are. This, along with the general expressions for ensemble-averaged error (2) and (9) and its minimization (12) are our main results.

*Conclusions.*—A universal bath-optimal minimal-energy control (BOMEC) of multidimensional decoherence has been introduced and shown to be a powerful tool, capable of facilitating new implementations of coherent control and quantum information processing. The analysis has yielded several conceptual innovations: (a) We have expressed an arbitrary gate error as the mean system-bath interaction energy. (b) Its multidimensional minimization has been expressed as the spectral overlap between the driven-system and the bath spectra. This formulation overcomes the long-standing conceptual obstacle of simultaneously controlling noncommuting system operators subject to noise along orthogonal axes. (c) Our Euler-Lagrange equation and its solution maximize the gate fidelity by anticorrelating the system and non-Markovian bath spectra. Hence, while DD-based methods rely on shifting the entire spectrum of the system beyond that of the bath, our approach takes advantage of commonly encountered gaps or dips of bosonic- or certain realistic spin-bath spectra [16–18]. Consequently BOMEC can be orders of magnitude lower in terms of energy investment than DD-based methods. Such energy saving may yield much higher fidelity, as excessive energies lead to leakage into additional levels [14,15], or increase the control noise [6]. By virtue of its generality, the present formulation may be expanded to quantum information tasks such as entanglement protection and manipulation under both local and global decoherence [13].

The support of EC (MIDAS), ISF and the von Humboldt Foundation (G. K.) is acknowledged.

[1] J. Fischer and D. Loss, Science **324**, 1277 (2009).
[2] L. Viola and S. Lloyd, Phys. Rev. A **58**, 2733 (1998); D. Vitali and P. Tombesi, Phys. Rev. A **59**, 4178 (1999); G. S. Agarwal, Phys. Rev. A **61**, 013809 (1999); L. Viola, E. Knill, and S. Lloyd, Phys. Rev. Lett. **82**, 2417 (1999); L. Viola and E. Knill, Phys. Rev. Lett. **90**, 037901 (2003); K. Khodjasteh and L. Viola, Phys. Rev. Lett. **102**, 080501 (2009); K. Khodjasteh and L. Viola, Phys. Rev. A **80**, 032314 (2009); K. Khodjasteh, D. A. Lidar, and L. Viola, arXiv:0908.1526.
[3] K. Khodjasteh and D. A. Lidar, Phys. Rev. Lett. **95**, 180501 (2005); K. Khodjasteh and D. A. Lidar, Phys. Rev. A **75**, 062310 (2007); J. R. West, B. H. Fong, and D. A. Lidar, arXiv:0908.4490.
[4] G. S. Uhrig, Phys. Rev. Lett. **98**, 100504 (2007); **102**, 120502 (2009); M. J. Biercuk *et al.*, Nature (London) **458**, 996 (2009).
[5] A. G. Kofman and G. Kurizki, Phys. Rev. Lett. **87**, 270405 (2001); Phys. Rev. Lett. **93**, 130406 (2004); IEEE Trans. Nanotechnol. **4**, 116 (2005).
[6] Y. Sagi, I. Almog, and N. Davidson, arXiv:0905.0286.
[7] G. Gordon, G. Kurizk, and D. A. Lidar, Phys. Rev. Lett. **101**, 010403 (2008).
[8] J. Clausen, G. Bensky, and G. Kurizki, arXiv:0909.1680.
[9] G. Gordon, N. Erez, and G. Kurizki, J. Phys. B **40**, S75 (2007).
[10] H.-P. Breuer and F. Petruccione, *The Theory of Open Quantum Systems* (Oxford University Press, Oxford, 2002).
[11] See supplementary material at http://link.aps.org/supplemental/10.1103/PhysRevLett.104.040401 for a derivation of Eq. (2).
[12] L.-A. Wu, P. Zanardi, and D. A. Lidar, Phys. Rev. Lett. **95**, 130501 (2005).
[13] G. Gordon and G. Kurizki, Phys. Rev. Lett. **97**, 110503 (2006).
[14] L.-A. Wu, G. Kurizki, and P. Brumer, Phys. Rev. Lett. **102**, 080405 (2009).
[15] G. S. Agarwal, Phys. Rev. A **54**, R3734 (1996).
[16] S. Kleff, S. Kehrein, and J. von Delft, Phys. Rev. B **70**, 014516 (2004); M. J. Storcz *et al.*, Phys. Rev. B **72**, 235321 (2005).
[17] Z. Lü and H. Zheng, J. Chem. Phys. **131**, 134503 (2009).
[18] N. V. Prokof'ev and P. C. E. Stamp, Rep. Prog. Phys. **63**, 669 (2000).